

ANALYSIS OF SCHRÖDINGER BASIN USING MOON MINERALOGY MAPPER SPECTRA G. Y. Kramer<sup>1†</sup>, D. A. Kring<sup>1</sup>, C. M. Pieters<sup>2</sup>, J. W. Head III<sup>2</sup>, P. J. Isaacson<sup>2</sup>, R. L. Klima<sup>3</sup>, T. B. McCord<sup>4</sup>, J. W. Nettles<sup>2</sup>, N. E. Petro<sup>5</sup>, <sup>1</sup>Lunar Planet. Inst., Houston, TX, <sup>2</sup>Brown Univ., Providence, RI, <sup>3</sup>Appl. Phys. Lab., Laurel, MD, <sup>4</sup>Bear Fight Center, Winthrop, WA, <sup>5</sup>Goddard SFC, Greenbelt, MD, <sup>†</sup>kramer@lpi.usra.edu

**Introduction:** Schrödinger Basin is ~320 km in diameter and located within the oldest and largest lunar basin, South Pole-Aitken (SPA). Schrödinger is one of the youngest lunar basins, only marginally older than Orientale [1,2]. This basin has been targeted as an ideal location for a future landing site [3] since it is thought to have tapped deep crustal lithologies associated with the SPA basin-forming event, contain ejected lithologies from the Orientale basin-forming event, and has volcanic materials in later mare and/or pyroclastic eruptions on its floor.

Here we present our first efforts (Fig. 1) to characterize Schrödinger's basin floor, peak ring, and basin rim materials using new spectral data from the Moon Mineralogy Mapper (M<sup>3</sup>). This analysis is compared with contemporary geologic maps and interpretations [2,4], which utilized Clementine UVVIS data. Nomenclature used in Figure 1 borrow from or modify that of [2]. We also look to find evidence in M<sup>3</sup> spectra of olivine and crystalline plagioclase in Schrödinger's peak ring, as recently observed in Kaguya data [5,6].

**Data & Processing:** M<sup>3</sup> mosaics created for this analysis used "K" calibrated radiance data [7], which was converted to apparent reflectance by removing the solar irradiance spectrum at the lunar surface. Schrödinger is located at high latitudes, which means illumination conditions are less than ideal for imaging spectroscopy measurements. At these latitudes there are low signal levels as a result of the low sun angle. This causes increased noise levels in reflectance spectra, and greatly complicates identification of mineralogically diagnostic absorption features. The best locations from which data can be extracted and still exhibit identifiable spectral features are in the sun-facing sides of crater walls and slopes.

Sampling from small, fresh craters provides a means to observe optically immature regions that exhibit strong absorption features, which are representative of the pristine lithology beneath the mature regolith blanket. These immature spectra are compared with spectra sampled from outside (but adjacent to) the fresh crater to observe whether the spectra are consistent with a single, maturing lithology, or if the spectra represent different materials. Spectra compared in this way indicate Schrödinger's basin floor is composed of local materials; consistent with the conclusions of [4] based on albedo contrast in Clementine data.

It is known that K calibration of M<sup>3</sup> data still contains several artifacts that produce systematic spectral errors (e.g., scattered light, minor non-linearity). These issues will be minimized in subsequent calibrations, such as that will be delivered to the PDS next June.

**Results:** With one exception, all sampled spectra exhibit broad, concave continuum slopes through the NIR wavelengths (Fig. 2), and lack an increasing

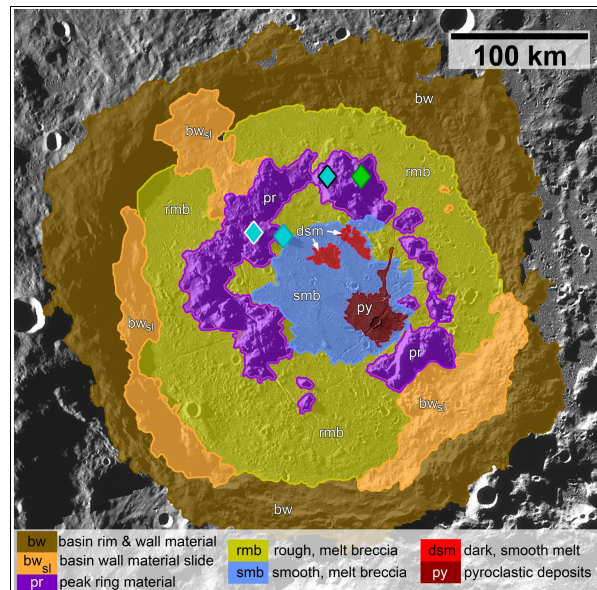


Figure 1: Geologic map of Schrödinger based on geomorphology & M<sup>3</sup> reflectance spectra. Diamonds show locations of olivine- and anorthosite-rich spectra shown in Fig. 2a.

spectral slope past 2200 nm due to thermal emission. The exception is the sun-facing slope of the pyroclastic vent (Fig. 1). Virtually all of the basin floor, rim, and peak ring materials exhibit unmistakable hydroxyl absorption features (Figs. 2), [8,9,10] testifying to the prevalence of OH in the polar regions.

The two major basin floor terrains are spectrally indistinguishable, and are consistent with a melt-rich breccia or impact melt, based on these preliminary analyses. Variation among locally sampled spectra consistently show a decreasing albedo associated with decreasing absorption band depth and increasing continuum slope, which we attribute to increasing maturity. Variation in the location of the maximum absorption near 1  $\mu$ m provides evidence of variable pyroxene compositions.

There are two dark mantle units within Schrödinger's peak ring, the northern unit, dsm, and pyroclastic deposits, unit py, which originate from a volcanic vent (Fig. 3). Unit py exhibits a characteristically glassy spectrum - low albedo, broad and weak mafic absorption features, and a steep, linear continuum slope [11]. These glassy spectral characteristics are particularly well demonstrated in the spectrum sampled from the sun-facing slope of the volcanic vent (Fig. 3b), which represents the pristine lithology. Spectra from small, young craters in unit py have low albedos and closely resemble those of dsm (Fig. 3a), although the 1  $\mu$ m absorption feature, attributed to pyroxene, shows wider variation in the position of its maximum absorption, suggesting a more variable calcium content. Both units dsm and py have a significant OH absorption near 2.8  $\mu$ m, although less relative to the surrounding basin floor.

Although distinct from those of the surrounding smooth melt breccia based on their slightly lower albedo, spectra from unit dsm do not appear consistent with the mare basalt interpretation of [2] and [4]. A mare basalt would exhibit more pronounced 1 and 2  $\mu\text{m}$  absorptions, and better defined 2  $\mu\text{m}$  maximum absorption. Spectra in dsm have a characteristic glassy spectral profile, and are similar to the smooth and rough impact melt breccia that comprise most of the basin floor with 2 exceptions: 1) a lower overall albedo, and 2) a continuum that is easily modeled by a straight line (in contrast to the concave continuum described above). As a unit, dsm is petrologically distinct from the pyroclastic deposits, py. The shallow 1  $\mu\text{m}$  absorption exhibited in surface and small crater spectra all have maximums near 1000 nm, which is characteristic of high-Ca pyroxene.

Our preliminary analysis of the basin rim and peak ring materials did not find exposures of >98% anorthite or definitive olivine spectral signatures as observed in Kaguya data [5,6]. However, we did find isolated locations in the peak ring (diamonds in Fig. 1), whose spectra (Fig. 2a,b) differ from the ubiquitous highland and mafic breccia signatures. The spectrum that looks to be olivine-rich exhibits a broad 1  $\mu\text{m}$  absorption feature, which may extend out to 1400 nm. However, the spectrum shows a slight absorption just shy of 2  $\mu\text{m}$ , indicating the presence of low-Ca pyroxene. The turquoise diamonds in Fig. 1 show the location of spectra that exhibit two distinct absorption features, one with a maximum near 1000 nm, indicating the presence of pyroxene, and the second near 1300 nm (Fig. 2b) possibly attributed to crystalline plagioclase. We found no spectrum without the accompanying 1000 nm absorption.

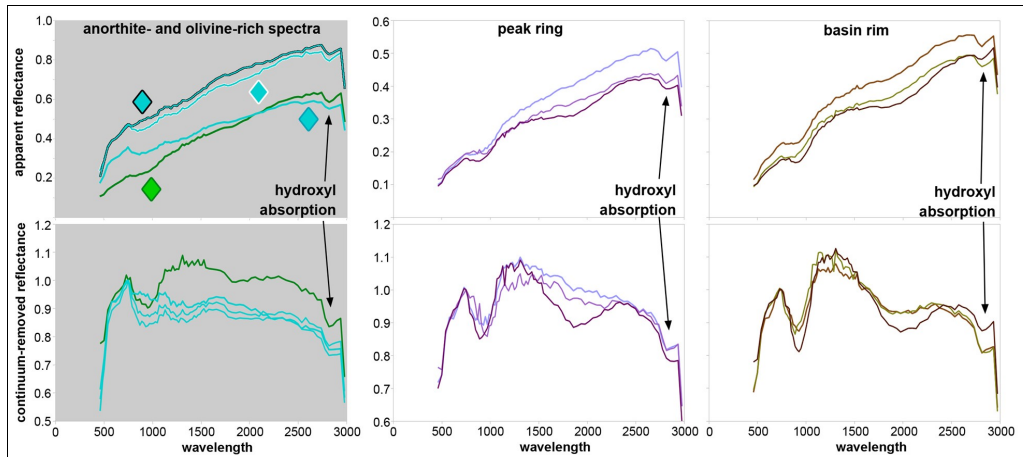


Figure 2: (a) Locations of reflectance spectra showing possible isolated anorthite- and olivine-rich exposures in Schrödinger's peak ring. (c) Spectra from fresh exposures in Schrödinger's peak ring and (e) basin rim. Bottom row of plots are the continuum-removed versions of the top row. Straight-line continuum calculated using the albedos at 750 nm and 2610 nm in the top row plots.

Our inability to confirm the pure anorthite and olivine-rich exposures observed in Kaguya spectral data [5,6] does not disprove either observation. Pure anorthite was resolved in Kaguya's Multi-Band Imager (MI), which although of lower spectral resolution and breadth, can spatially resolve a 62 m object. Thus, the MI may be distinguishing a pure anorthite that M<sup>3</sup> is mixing with another, adjacent lithology. The olivine signatures observed by Kaguya's Spectral Profiler (SP) are less easily explained, as SP is a point spectrometer with similar spectral and spatial resolution to M<sup>3</sup>.

Fresh material exposed in small, young craters in Schrödinger's basin rim reveal a significantly more crystalline material than the basin floor, based on the stronger absorption features in the spectra (Fig. 2e,f). The basin rim mineralogy is dominated by Ca-rich pyroxene, such as augite. We found no evidence of olivine or crystalline plagioclase in the basin rim. Fresh exposures in Schrödinger's peak ring (Fig. 2c,d) show spectral features of both low- and high-Ca pyroxenes.

REFERENCES: [1] Wilhelms *USGS Prof. Paper*, 1348, 1987. [2] Shoemaker et al. *Science*, 266, 1994. [3] Sullivan et al. *GSA Special Pub.*, (in press). [4] Shankar et al. *LPSC*, 41, 2010. [5] Ohtake et al. *Nature*, 461, 2009. [6] Yamamoto et al. *Nat. Geosci.*, 3, 2010. [7] Green et al. *J. Geophys. Res.*, (in review) [8] Pieters et al. *Science*, 326, 2009. [9] Clark *Science*, 326, 2009. [10] Sunshine et al. *Science*, 326, 2009. [11] Tompkins & Pieters. *Meteor. Planet. Sci.*, 45, 2010.

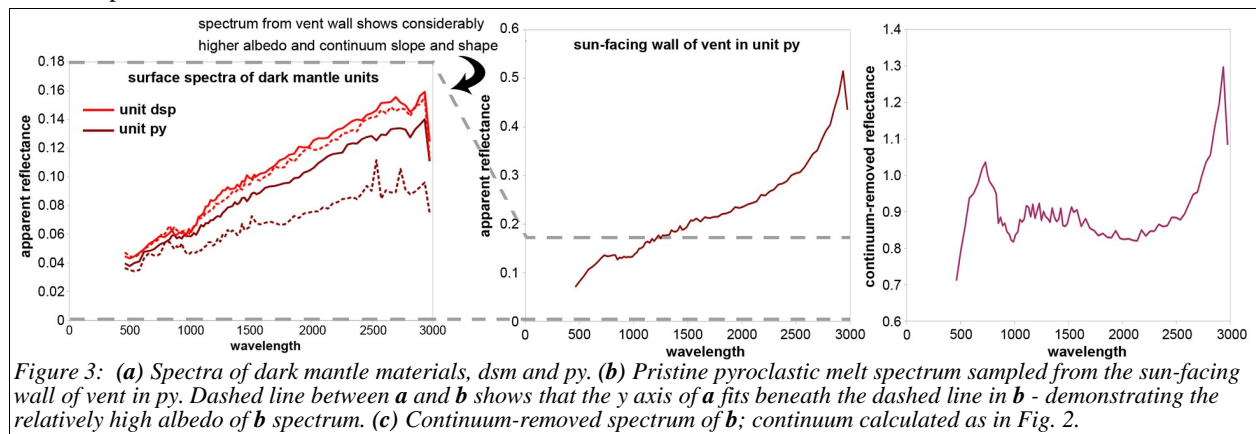


Figure 3: (a) Spectra of dark mantle materials, dsm and py. (b) Pristine pyroclastic melt spectrum sampled from the sun-facing wall of vent in py. Dashed line between a and b shows that the y axis of a fits beneath the dashed line in b - demonstrating the relatively high albedo of b spectrum. (c) Continuum-removed spectrum of b; continuum calculated as in Fig. 2.